

Numerical Investigation of the Mixing of Highly Viscous Liquids with Cowles Impellers

Matteo Antognoli, Chiara Galletti, Riccardo Bacci di Capaci*, Gabriele Pannocchia, Claudio Scali

Department of Civil and Industrial Engineering, University of Pisa, Largo Lucio Lazzarino 2, 561226, Pisa, Italy
riccardo.bacci@ing.unipi.it

This work is aimed at investigating the mixing process of highly viscous paints, used to colour leathers in the tanning industry, through Computational Fluid Dynamics (CFD). In particular, a mixing tank is fed with a master liquid and different liquid pigments and then stirred by Cowles impellers in order to obtain a paint of a uniform colour. The typical dynamic viscosity of the liquids in this process is $\mu \sim O(0.1-10)$ Pa·s, while the Cowles rotational speed is usually very high, i.e. 3000-5000 rpm.

The numerical model is based on the solution of the unsteady Reynolds-Averaged Navier–Stokes (RANS) equations for continuity, momentum and species mass fractions, the latter being used to describe the different components. The impeller motion is modelled through the Sliding Deforming Mesh (SDM) approach, using rotating (unstructured) meshes in the impeller region and a static (structured) mesh in the remainder of the tank. The master liquid and coloured pigments are assumed to stratify within the tank at initial time and the steady rotational speed is then imposed abruptly to the impellers.

The level of homogeneity in the stirred tank is evaluated through the analysis of component concentration fields over time. In particular, such local concentrations can be used to determine the mixture colour in different regions of the tank, and hence predict the degree of homogeneity at different times; this is accomplished by defining a proper homogeneity indicator based on the spatial variance of the estimated colour. The proposed numerical model provides an efficient method to investigate the colour of the mixture and to evaluate an appropriate mixing time. The methodology gives also important indications for the tank design, especially useful in the case of non-conventional impellers, high rotation rates and viscous fluids.

1. Introduction

Mixing processes are one of the most important and common operations in the process industry. In general, the equipment used is stirred tank, which allows one to achieve an efficient blending of liquids and to add and disperse solids. Storage operations also require stirred tanks to avoid particle sedimentation in order to preserve original mixture properties. In particular, the tanning industry is one of the industrial areas, like pharmaceutical, polymer, speciality and food (Paul et al., 2004), which processes highly viscous fluids. Typically, liquid paints based on synthetic or natural resins and cellulose, combined with dyed pigments are used with the specific aim of colouring leathers. In this context, non-Newtonian and highly viscous fluids (0.1 - 10 Pa·s) are involved; High Shear Impellers (HSI), i.e. sawteeth and Cowles, are needed, and significant amounts of energy due to very high rotation rates are required in order to achieve mixture homogenization in acceptable times. Thus, blending and dispersion processes require good control and reliable prediction of the properties (i.e. viscosity and colour) of the desired mixture to obtain a replicable and quality product.

Many works were focused on the prediction of mixing time and physical properties of viscous fluids in turbulent regimes with different HSI and for various geometrical configurations. For example, Martínez-de Jesús et al. (2018) presented a detailed hydrodynamic characterization in the transitional flow regime of two variants of Norstone Polyblade. Viscous dissipation and effective circulation were used as key parameters to assess and compare the performance of different HSI impellers.

Generally speaking, Computational Fluid Dynamics (CFD) studies are conducted to describe monophasic or multiphase systems in stirred tanks (Molnar et al, 2013; Zhang et al., 2013). CFD numerical simulations model impeller motion by defining a dynamic numerical domain. In particular, there are three main methods to handle impeller motion: Moving Reference Frame (MFR), Sliding Mesh, and Sliding Deforming Mesh (SDM), the latter being precisely described by Yeoh et al. (2004). As for turbulence, the two most common approaches are based on Large-Eddy Simulation (LES) and Reynolds-Averaged Navier Stokes (RANS) equations, being Direct Numerical Simulations generally too expensive. Zadghaffari et al. (2010) presented LES of the mixing process in a baffled tank, where impeller rotation was modelled using Sliding Mesh technique. The results proved LES a reliable tool to investigate the unsteady behaviour of turbulent flow in stirred vessel; LES was also found to be able to identify macro-instabilities (Galletti et al., 2005). On the other hand, RANS approach can adopt many turbulence models (Jones et al., 2001) and requires shorter computation times, but usually proves less accurate than LES model (Yeoh et al., 2004). However, RANS approach is confirmed very useful: Buwa et al. (2006) predicted power consumption and mixing time by CFD simulation with RANS approach in good agreement with experimental measurements.

The present work is aimed at developing a CFD numerical model of the mixing process of different highly viscous components, i.e. master liquid and coloured pigments, in a tank stirred by two Cowles impellers at high rotation rate, which represents a hardly investigated scenario, but typical of the processes of mixing in the tanning industry. A bespoke subroutine is used to estimate the RGB colour of the viscous mixture from local values of component concentration and thus to allow the computation of mixing time.

2. Modelling approach

2.1 Tank configuration

An unbaffled vessel with an inner diameter $T = 0.520$ m and a height $H = 0.930$ m was considered. The bottom had a semi-elliptical shape. The tank volume, approximately 210 L, was filled with viscous coloured fluids. The tank was equipped with two Cowles impellers, both having a diameter $D = T/3 = 0.173$ m. Each impeller presented twelve pairs of teeth of height $h = D/10$ inclined by $\alpha = 15^\circ$ from the vertical axis. The impeller thickness was assumed to be zero for the sake of simplicity. The round-bottom configuration and the small clearance left by the lower impeller ($C = 0.100$ m) allowed one to strongly reduce sedimentation and fouling phenomena possible due to the high-density pigments within the paint. The distance between the two Cowles impellers was $H/2 = 0.465$ m and the shaft had diameter $d = 0.040$ m. The agitation speed of the two impellers was $N = 3000$ rpm to guarantee a good dispersion and an intense mixing. The impellers were equipped with dampers to reduce vibrations of the driveshaft.

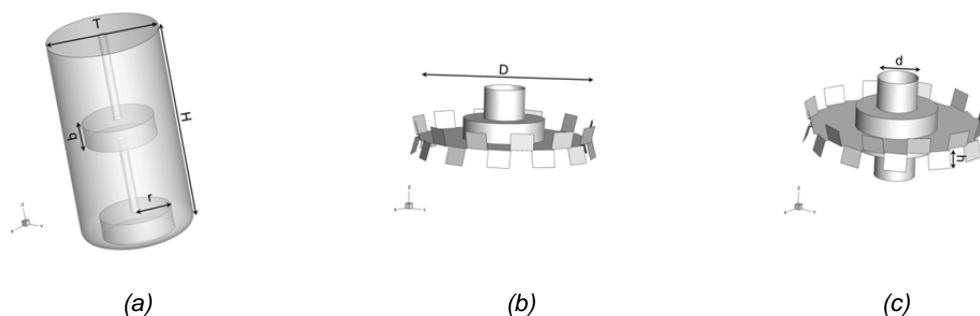


Figure 1: (a) 3D representation of the tank and Cowles impellers: (b) lower and (c) upper.







2.2 Operating conditions

The process aimed at the mixing of five components to create a specific formulation used by the tanning industry for painting leather. Four components were liquid pigments, while the fifth was a master liquid able to dissolve each element. Table 1 lists concentration, physical properties and RGB colours of each component and the final mixture. Interactions between components are known to be non-ideal, as the mixture tends to develop high-viscosity spots and may sometimes clog the impellers motion. Nevertheless, for the sake of simplicity, component interactions were here assumed ideal and, furthermore, physical properties, i.e. density and viscosity, were linearly weighted on the mass fractions of components.

Since the aim of the numerical model was to provide an estimation of the mixing time, at the beginning of the simulation the components were assumed to be stratified, as shown in Figure 2a. In this condition of perfect segregation, the white-ochre, component in largest quantity, lays on the tank bottom, while the other pigments

are present in traces on the top. The simulation lasted up to achieving the mixing time (t_{mix}), defined as the time when the concentration of components is floating around the stationary value by less than 2.5%. The achieving of mixing time was verified by time trends of the mass concentration of orange pigment measured by three point-probes (Figure 2b).

Table 1: List of components with concentrations, physical properties and RGB values.

Component	Concentration [g/kg]	Viscosity [Pa·s]	Density [kg/m ³]	RGB	
White-ochre	500.35	0.2746	1,122.23	[204 119 34]	
Blue	10.00	0.4927	1,052.35	[0 0 255]	
Black	8.00	0.5871	1,038.80	[0 0 0]	
Orange	25.35	2.3090	1,005.20	[255 127 0]	
Master liquid	456.30	0.6883	1,050.40	[220 220 220]	
Mixture	1000.00	0.5210	1,085	[221.71 197.20 175.25]	

The fluid dynamics of flow in the stirred tank was dependent on the Reynolds number:

$$Re = \frac{\rho ND^2}{\mu} = 3,116 \quad (1)$$

Where ρ , μ are density and dynamic viscosity of the mixture, N and D are rotational speed and diameter of the impellers. Note that, despite the high agitation rate, Re fell within the transition region between laminar and turbulent regimes because of the high weighted-average viscosity.

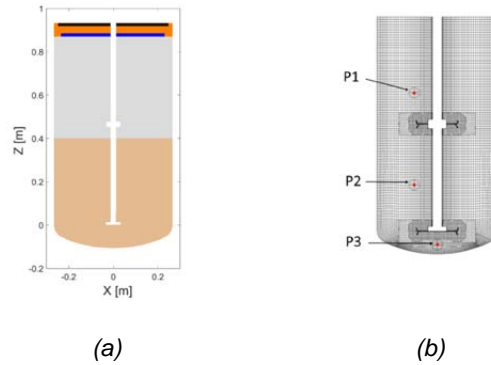


Figure 2: (a) Initial condition of the numerical simulation with components in real colours stratified along the Y-section; (b) Mesh on XZ-plane with the location of three concentration point-probes.

3. Computation method and numerical simulations

3.1 RANS model

The governing equations were solved using the well-established commercial CFD solver Fluent 19.2 (ANSYS Inc.). The Reynolds-Averaged Navier Stokes (RANS) equations were combined with transport equations for $n-1$ components, where n is the number of species detailed in Table 1. Reynolds stress equation was closed through the $k-\omega$ Shear Stress Transport (SST). The SIMPLE algorithm was used for the pressure-velocity coupling and the transient formulation was set with a second order implicit integration method with a time-step of $3.0 \cdot 10^{-4}$ s, ensuring a Courant number $C < 10$.

3.2 Sliding Deforming Mesh method

The Sliding Deforming Mesh (SDM) was applied to describe the fluid dynamic behaviour induced by impellers motion. Basically, the computation domain was split into three parts: two zones were the Dynamic Meshes (DMs) formed by two cylindrical discs of radius r able to rotate consistent with two impellers while the remaining volume, called Static Mesh (SM), was perfectly steady. The DMs were mainly comprised of polyhedral cells able to model the complex surfaces of Cowles impeller, while a structured grid formed by hexahedron elements was used for the SM (see Figure 2b). Overlapped interfaces were defined as boundary conditions between the two types of domain. Thus, two DMs were able to slide on the SM along interfaces time-step by time-step. Despite meshes had different grids, the connectivity between cells of two different domains was re-established every time the sliding occurs. The size of two cylindrical domains was set with a

ratio $r/T = 0.32$ (Yeoh et al., 2004) and a vertical extension of $b = 0.100$ m, that is, about 2.5 times the blade height (Coroneo et al., 2011).

3.3 Mesh analysis

A grid independence study was preliminary performed using three different mesh sizes over a half-tank volume including only the bottom impeller. Hence, three maximum values for cell dimension (20, 14, 8 mm) were set to obtain three different grid densities (low, medium and high), corresponding to the following numbers of elements per grid: 247,985; 542,551 and 883,740. Each grid was generated to provide a $y^+ < 5$. A near-wall approach was used to describe turbulence effects in the proximity of tank walls and impeller surfaces. The smallest cell dimension was set to 1 mm. Figure 3 shows the comparison of normalized radial velocity u_r/u_{tip} and mass fraction of the master liquid for the three grid densities along X-coordinate at impeller height. Note that the origin is located at impeller centre. Medium and high-density grids yield similar profiles, but the low-density grid does not produce accurate results; therefore, the medium density grid was chosen leading to 990,158 cells when applied to the whole vessel to run complete CFD simulation. It is worth noting that a rigorous grid convergence study could not be carried out because a proper grid refinement index cannot be defined systematically, especially when using the available grid generation algorithms (Roache, 1994).

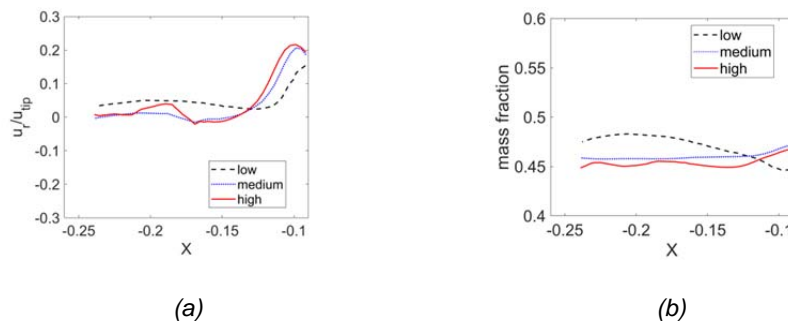


Figure 3: (a) Normalized radial velocity and (b) mass fraction of the master liquid at impeller plane along X-coordinate ($-0.24 \text{ m} < X < -0.09 \text{ m}$.) at time 0.12 s for three different mesh density.

3.4 RGB investigation

Finally, a post-processing analysis was performed with a MATLAB[®] routine to describe the mixture colour and its standard deviation over time according to the RGB model. The input data were component concentration values and cell volumes. At each simulation time, the routine computed RGB colours on XZ-plane and colour standard deviation σ over the whole tank domain as:

$$RGB_i = \sum_j^n RGB_j \cdot x_{ij} \quad (2)$$

$$\sigma = \sqrt{\frac{1}{N_{cell}} \sum_i^{N_{cell}} (RGB_i - \overline{RGB})^2} \quad (3)$$

where x_{ij} is the mass fraction of the j -th component in the i -th cell, RGB_j are components colour (see Table 1), \overline{RGB} is the mixture colour weighted-average over the volume of cells and N_{cell} is the number of cells.

4. Results and Discussion

4.1 CFD simulation results

The mass fraction field of components was evaluated on XZ-plane at different times. Results for orange pigment and master liquid are reported in Figure 4. At time $t = 0$, the master liquid is stratified in the middle of the tank (Figure 4a). As agitation starts, the initial configuration is broken: all the bulk of master liquid moves upwards (Figure 4b) and then undergoes significant convective flow. The component is indeed forced to move downwards along the axial direction until reaching the tank bottom (Figures 4c and 4d). Figures 4g-l show the mass fraction field of the orange component at the same six time instants. Note that in this case, the colour bar amplitude tightens over time. The agitation firstly creates a central descendent flow inducing a quick shift of orange pigment and then a fast dispersion once the component reaches the top impeller surface (see

Figure 4h and 4i). As a matter of fact, an efficient mixing mechanism with evident turbulent vortices is established which is able to push orange pigment towards bottom region as shown in Figures 4j and 4l. Overall, it has to be observed that all tank regions are effectively involved in the mixing process until uniform concentrations are achieved (see Figure 4f).

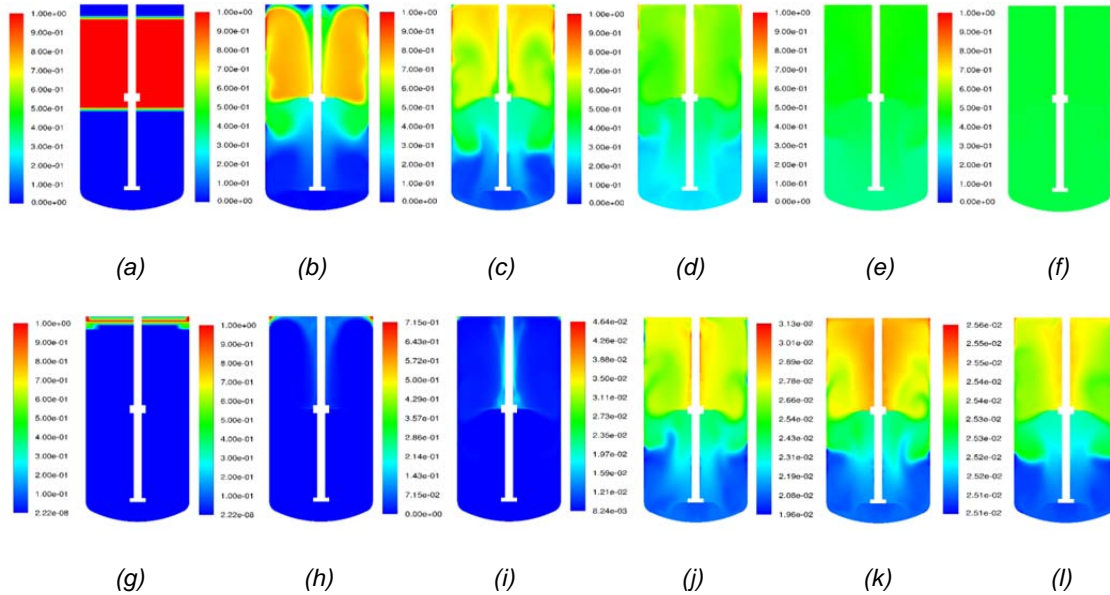


Figure 4: Mass fraction field of master liquid (a-f) and orange component (g-l) on ZX-plane at time: (a,g) 0 s, (b,h) 0.6 s, (c,i) 1.2 s, (d,j) 2.4 s, (e,k) 4.8 s and (f,l) 10.6 s.

Moreover, the molar concentration of orange pigment was recorded over time through the three probes of Figure 2b. The probe P1 was located above upper impeller at $(X,Y,Z) = (-0.1,0,0.6)$; P2 is between the two impellers at $(X,Y,Z) = (-0.1,0,0.2)$; P3 is placed under the bottom impeller at $(X,Y,Z) = (0,0,-0.07)$. Figure 5a shows time trends normalized over the stationary concentration C_{∞} . Trends measured by P1 and P2 appear very fluctuating as typical for turbulent behaviour. Finally, the mixing time can be evaluated equal to 10.6 s.

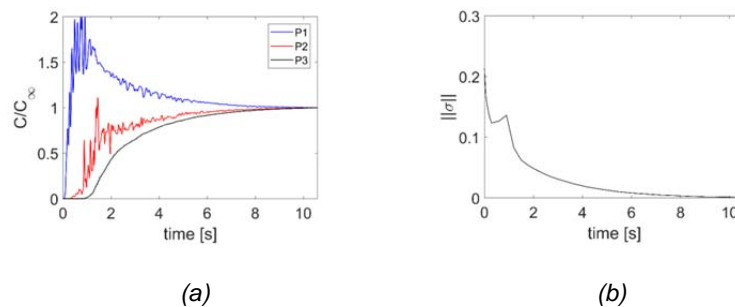


Figure 5: (a) Normalized concentration of orange component and (b) standard deviation norm of RGB colours.

4.2 Colour analysis

The module of the standard deviation $\|\sigma\|$ of RGB values was computed using data collected from CFD concentration fields at different time instants. This index proved high for the initial condition of colour segregation and tended to zero once the system was perfectly mixed, that is, when $t \rightarrow t_{mix}$ (see Figure 5b). Note that the mixing time value registered by the three probes was here confirmed on the basis of time trend of $\|\sigma\|$. Moreover, Figure 6 compares the distribution of RGB colours on XZ-plane at different simulation times. In particular, Figure 6a reveals that black pigment is not immediately involved in convection flows. Note that the subsequent fast drop of black pigment (Figure 6b) temporarily increases the colour standard deviation as shown in Figure 5b. However, it is worth observing that results from Figure 6 are in solid agreement with observations from Figure 4b-f and g-l, since a perfect mixing is achieved in 10.6 s. Furthermore, Figure 6 shows a realistic simulation of paints and allows one to appreciate the colour quality of the mixture achieved.

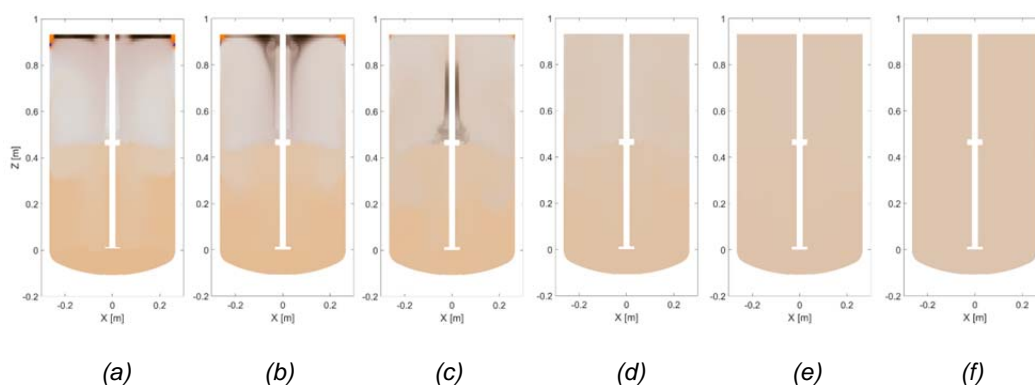


Figure 6: RGB field on ZX-plane at time: (a) 0.3 s, (b) 0.6 s, (c) 1.2 s, (d) 2.4 s, (e) 4.8 s and (f) 10.6 s.

5. Conclusions

In the present work, Computational Fluid Dynamics was used to investigate the mixing process of highly viscous paints for the tanning industry. The numerical concentration fields were post-processed by using a RGB analysis to determine the colour of the mixture. Moreover, the standard deviation of such RGB colour was estimated across the vessel to determine the mixing time. Results were encouraging and allowed understanding the mixing process of the pigments, although the computational cost of the simulations was found to be very high due to the small time-step needed to capture the transient behaviour in presence of very high rotational speed. Future works will be devoted at investigating the effect of operating and geometrical conditions such as rotational speed and position of the impellers.

Acknowledgments

This work has been supported by Sviluppo Regione Toscana through the POR FESR 2014 - 2020 funding program (Tintometro Robotizzato per Conceria - True Colors).

References

- Buwa V., Dewan A., Nassar A.F., Durst F., 2006, Fluid dynamics and mixing of single-phase flow in a stirred vessel with a grid disc impeller: Experimental and numerical investigations. *Chemical Engineering Science*, 61, 2815–2822.
- Coroneo M., Montante G., Paglianti A., Magelli F., 2011, CFD prediction of fluid flow and mixing in stirred tanks: Numerical issues about the RANS simulations, *Computers & Chemical Engineering* 35, 1959–1968.
- Galletti, C., Paglianti, A., Yianneskis, M., 2005, Observations on the significance of instabilities turbulence and intermittent motions on fluid mixing processes in stirred reactors, *Chemical Engineering Science*, 60, 2317–2331.
- Martínez-de Jesús G., Ramírez-Muñoz J., García-Cortés D., Cota L.G., 2018, Computational fluid dynamics study of flow induced by a grooved high-shear impeller in an unbaffled tank, *Chemical Engineering and Technology*, 41, 580–589.
- Molnár B., Egedy A., Varga T., 2013, CFD model based comparison of mixing efficiency of different impeller geometries. *Chemical Engineering Transactions*, 57, 1441–1446.
- Jones R.M., Harvey III A.D., Acharya S., 2001, Two-equation turbulence modelling for impeller stirred tanks. *Journal of Fluids Engineering*, 123, 640-648.
- Paul E.L., Atiemo-Obeng V.A., Kresta S.M., 2004, *Handbook of industrial mixing: Science and practice*. John Wiley & Sons Inc., New Jersey, USA.
- Roache P.J., 1994, Perspective: A method for uniform reporting of grid refinement studies. *Journal of Fluids Engineering*, 116, 405–413.
- Yeoh S.L., Papadakis G., Lee K.C., Yianneskis M., 2004, Numerical simulation of turbulent flow characteristics in a stirred vessel using the LES and RANS approaches with the sliding/deforming mesh methodology, *Chemical Engineering Research and Design*, 82, 834–848.
- Zadghaffari R., Moghaddas J.S., Revstedt J., 2010, Large-eddy simulation of turbulent flow in a stirred tank driven by a Rushton turbine, *Computers & Fluids* 39, 1183–1190
- Zhang S., Müller D., Arellano-Garcia H., Wozny G., 2013, CFD simulation of the fluid hydrodynamics in a continuous stirred-tank reactor, *Chemical Engineering Transactions*, 57, 1441–1446.